Title

Performance evaluation of V_{SZ}-to-V_{S30} correlation methods using global V_S profile database

Authors

Kwak, Dong Youp
Ancheta, Timothy D
Mitra, Devjyoti
et al.

Publication Date

2017-07-01

Peer reviewed

Performance evaluation of V_{SZ}-to-V_{S30} correlation methods using global V_S profile database

Dong Youp Kwak, Timothy D. Ancheta & Devjyoti Mitra
RMS, Inc., Newark, California, USA
Sean K. Ahdi, Paolo Zimmaro, Grace A. Parker, Scott J. Brandenberg & Jonathan P. Stewart
Department of Civil and Environmental Engineering – University of California, Los Angeles, California, USA

ABSTRACT
The time-averaged shear wave velocity in the upper 30 m (V_{S30}) is commonly used as explanatory variable for site characterization. Although measuring shear wave velocity (V_S) to 30 m or greater depth is the most direct and robust way to compute V_{S30}, oftentimes V_S profiles are shallower than 30 m. For such cases, various methods have been proposed to extrapolate the time-averaged V_S to a specified depth (V_{SZ}) and/or V_S at a specified depth to V_{S30}. These V_{SZ}-to-V_{S30} extrapolation methods typically provide a greater predictive power than methods based on geotechnical investigation (e.g., correlations with penetration resistance) and on proxies (e.g., surface geology, terrain categories, or topographic slope). In this study, we investigate the functional forms used in five V_{SZ}-to-V_{S30} extrapolation models: (1) Boore (2004), (2) Boore et al. (2011), (3) Midorikawa and Nogi (2015), (4) Dai et al. (2013), and (5) Wang and Wang (2015). We then validate model performances using five regional V_S profile datasets: (1) Japan - 289 profiles from the KiK-Net and PARI arrays; (2) California - 71 profiles from Caltrans reports; (3) Oregon and Washington - 450 profiles from reports of state and federal geologic surveys (Oregon DOGAMI, Washington DNR-GER, USGS, and CGS) and various studies performed by university research groups; (4) central and eastern North America - 200 profiles from the reports of Nuclear Regulatory Commission and university research group studies; (5) Beijing plain, China - 463 profiles from unpublished technical and research reports. For each selected model, we perform regression analyses developing model coefficients for those five datasets and then investigate potential regional differences. Midorikawa and Nogi (2015) and Dai et al. (2013) models provide the lowest model bias and dispersion relative to measured V_{S30} values. We also developed non-region-specific models which provide comparable model bias and dispersion to the region-specific models. The developed models are applicable to any V_S profile for depths < 30 m.

1 INTRODUCTION

The time-averaged shear wave velocity in the upper 30 m (V_{S30}) is a commonly used explanatory variable for site characterization in various applications such as: (1) ground motion modeling, (2) development of building codes, and (3) seismic hazard maps. V_{S30} is estimated using the following techniques (in order of preference): (1) in-situ seismic velocity measurements, (2) correlation models to soil penetration resistance [from standard penetration test blow count or cone penetration test tip resistance], and (3) proxy-based relationships (usually based on surface geology, terrain categories, or topographic slope). Although measuring shear wave velocity (V_S) to 30 m or greater depth is the most direct and robust way to compute V_{S30}, oftentimes V_S profiles are shallower than 30 m. For such cases, various methods have been proposed to extrapolate the time-averaged V_S to a specified depth (V_{SZ}) and/or V_S at a specified depth to V_{S30}. These V_{SZ}-to-V_{S30} extrapolation methods typically provide a greater predictive power than methods based on geotechnical investigation and on proxies (Seyhan et al., 2014; Parker et al., 2017).

In this study, we investigate five V_{SZ}-to-V_{S30} extrapolation methods: (1) Boore (2004); (2) Boore et al. (2011); (3) Midorikawa and Nogi (2015); (4) Dai et al. (2013); (5) Wang and Wang (2015), and evaluate relative performance of each method using a large V_S profile database (total of 1,466 profiles) covering California, Central and Eastern North America, Pacific Northwest, Japan, and China. Model coefficients for each method and region are developed through regression analyses. Non-region-specific model coefficients are also developed by combining the datasets using equal weight for each region. We specifically select available and widely used V_{SZ}-to-V_{S30} extrapolation models. We recognize that geotechnical models based on either laboratory test data or field investigation results (e.g. Cha et al., 2014) could be expanded and adapted to perform similar extrapolations, but we do not take this approach here.

2 DATA RESOURCES

Databases of V_S measurements for each region are:

- California (CA): a V_S profile data set collected at various California bridge sites (described by Brandenberg et al., 2010);
- Central and Eastern North America (CENA): reports of Nuclear Regulatory Commission and university research group studies as a part of NGA-East project (Parker et al., 2017);
- Pacific Northwest (PNW): reports of state and federal geologic surveys (Oregon DOGAMI, Washington DNR-GER, USGS, and CGS) and various studies performed by university research groups. This database is being used for NGA-

Subduction project (Ahdi et al., 201x);

- Japan (JP): profiles for seismic stations at Kiban Kyoshin Network (KiK-net) and Port and Airport Research Institute (PARI) (NIED, 2017; PARI, 2017);
- China (CN): a soil-profile database for the Beijing plain area from unpublished technical and research reports (Xie et al., 2016).

Table 1 summarizes data sources and the number of profiles for each region. Methods of V_S measurements are: suspension logging for CA; various body- and surface-wave techniques for CENA and PNW; and downhole for JP and CN. Figure 1 shows locations of all profiles.

Table 1. V_S profiles sources for each region

Region	Number of profiles	Sources
California	71	Brandenberg et al. (2010)
Pacific Northwest	450	Ahdi et al. (201x)
Central & East North America	200	Parker et al. (2017)
Japan	282	NIED (2017) and PARI (2017)
China	463	Xie et al. (2016)
Total	1466	

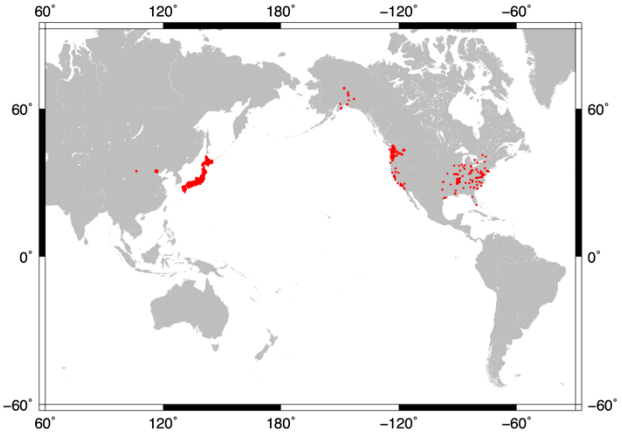

Figure 1. Locations of V_S profiles (red points) used in this study.

Histograms of V_{S30} for each region and all data sets are shown in Figure 2. The first histogram in Figure 2 shows the distribution of V_{S30} for the global data set compiled in this study. This global data set is approximately log-normally distributed with a geometric mean (μ) of 301 m/s and standard deviation of the natural logarithms of V_{S30} ($\sigma_{\ln V}$) of 0.47. As shown in Figure 2, the CA and CENA data sets have similar distributions to the global data set in terms of their mean and $\sigma_{\ln V}$. PNW and CN sites are softer on average, while JP sites are placed on stiff soil to hard rock sites producing a higher mean. Another notable feature is that the CN data set has a narrow distribution ($\sigma_{\ln V}$ = 0.15), which results from its sampling of a relatively small area (Beijing plain). The overwhelming majority of the profiles in this data set are located on Holocene alluvial and pluvial deposit (Xie et al., 2016).

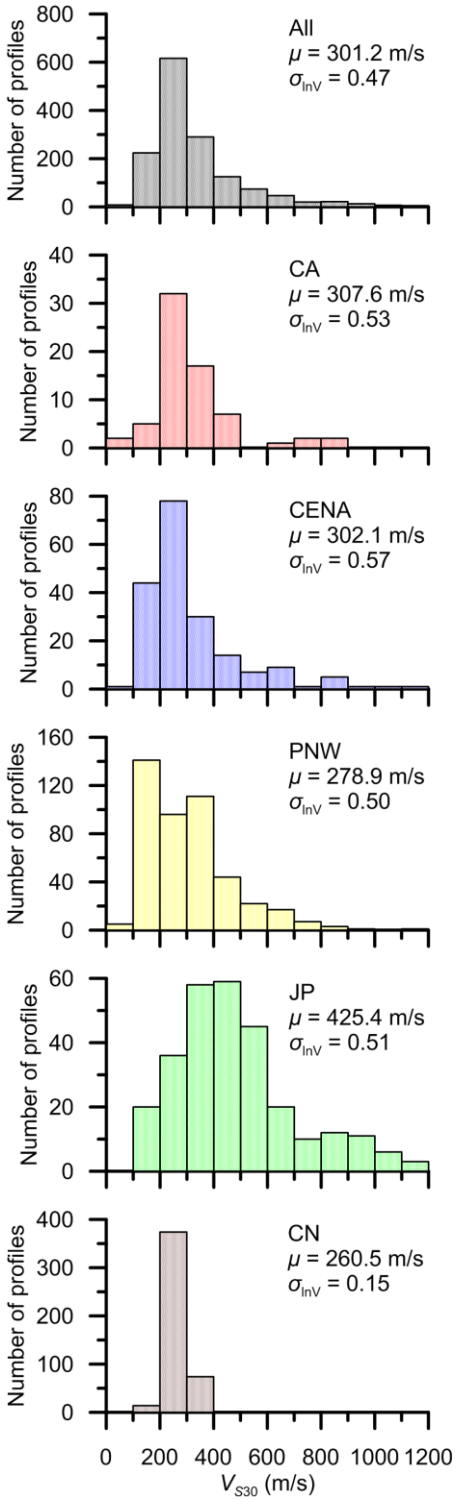

Figure 2. V_{S30} histograms for profiles used for California (CA), Central and Eastern North America (CENA), Pacific Northwest (PNW), Japan (JP), China (CN), and all

resources.

3 V_{S30} PREDICTION MODEL FOR V_S PROFILES WITH DEPTH LESS THAN 30 M

All profiles in this study extend to at least 30 m depth, which provides a means for assessing the accuracy of the V_{SZ}-to-V_{S30} extrapolations. We compute time-averaged shear wave velocities to depths z in the range from 5 to 29 m in 1 m increments. The resulting values of V_{SZ} are used as independent variables in five V_{SZ}-to-V_{S30} extrapolation methods to evaluate their performance. These extrapolation models are described below.

Boore (2004)

The first model considered is Boore (2004; hereafter B04), for which $\log(\widehat{V_{S30}})$ is a linear function of $\log(V_{SZ})$. Note that the hat on V_{S30} indicates a predicted mean value. B04 was originally developed from 135 boreholes in California. The model form is:

$$\log(\widehat{V_{S30}}) = c_0 + c_1 \log(V_{SZ}) \quad [1]$$

where c_0 and c_1 are model coefficients.

Boore et al (2011)

The second model considered in this study (Boore et al., 2011; hereafter Bea11) has a parabolic functional form, and it is based on data from 638 KiK-Net sites in Japan:

$$\log(\widehat{V_{S30}}) = c_0 + c_1 \log(V_{SZ}) + c_2 [\log(V_{SZ})]^2 \quad [2]$$

where c_0, c_1, and c_2 are model coefficients.

Midorikawa and Nogi (2015)

Midorikawa and Nogi (2015; hereafter MN15) data are from 2009 sites in Japan. This model considers V_{SZ} as well as V_S at the profile depth, $V_S(z)$, as follows:

$$\log(\widehat{V_{S30}}) = c_0 + c_1 \log(V_{SZ}) + c_2 \log(V_S(z)) \quad [3]$$

Table 2. Model coefficients developed for each region where c_0, c_1, and c_2 are model coefficients.

Dai et al (2013)

Dai et al (2013; hereafter Dea13) present an approach in which the travel time from the bottom of the profile to 30 m is estimated from $V_S(z)$. First, the time-averaged V_S from z to 30 m (V_{SZ30}) is estimated as follows:

$$\log(\widehat{V_{SZ30}}) = c_0 + c_1 \log(V_S(z)) \quad [4]$$

Next, V_{S30} is predicted as follows:

$$\widehat{V_{S30}} = \frac{30}{tt_z + \frac{30-z}{\widehat{V_{SZ30}}}} \quad [5]$$

where tt_z represents travel time from surface to profile depth (z). The $\widehat{V_{SZ30}}$ from Eq. [4] is used for the travel time computation over the depth range of z to 30 m in Eq. [5].

Wang and Wang (2015)

Wang and Wang (2015; hereafter WW15) use the following functional form:

$$\log(\widehat{V_{S30}}) = \log(V_{SZ2}) + \frac{\log 30 - \log z_2}{\log z_2 - \log z_1} \times [\log V_{SZ2} - \log V_{SZ1}] \quad [6]$$

where z_2 is the profile depth, $z_1 = z_2 - 3$ m (approach used here, other forms considered by Wang and Wang, 2015), and V_{SZ1} and V_{SZ2} are corresponding time-averaged velocities to z_1 and z_2. The closer z_2 is to 30 m, the greater correlation to measured V_{S30} and the smaller $\sigma_{\ln V}$ (Wang and Wang, 2015). No regression coefficients are required.

Regressions

For the first four methods, we develop region-specific model coefficients using the database from Section 2. Figure 3 shows model coefficients for each region for

Region		All			CA			CENA			PNW			JP			CN		
Model	z (m)	c_0	c_1	c_2	c_0	c_1	c_2	c_0	c_1	c_2	c_0	c_1	c_2	c_0	c_1	c_2	c_0	c_1	c_2
Boore 2004	5	0.474	0.879	-	0.567	0.815	-	0.411	0.903	-	0.648	0.793	-	0.452	0.930	-	0.806	0.714	-
	10	0.172	0.985	-	0.305	0.914	-	0.185	0.982	-	0.333	0.911	-	0.180	1.003	-	0.307	0.915	-
	15	0.083	1.003	-	0.217	0.939	-	0.112	0.995	-	0.164	0.966	-	0.086	1.014	-	0.114	0.983	-
	20	0.035	1.009	-	0.120	0.970	-	0.069	0.997	-	0.072	0.991	-	0.031	1.015	-	0.064	0.992	-
	25	0.009	1.007	-	0.037	0.994	-	0.031	0.999	-	0.020	1.001	-	0.009	1.009	-	0.023	1.000	-
Boore et al. 2011	5	0.806	0.596	0.060	2.000	-0.347	0.233	1.270	0.184	0.149	0.867	0.594	0.045	0.345	1.022	-0.020	6.790	-4.692	1.219
	10	0.590	0.637	0.072	1.704	-0.213	0.225	0.545	0.689	0.059	0.772	0.521	0.085	-0.431	1.507	-0.104	4.636	-2.860	0.822
	15	0.334	0.799	0.041	0.821	0.461	0.094	0.336	0.815	0.036	0.644	0.552	0.089	-0.421	1.423	-0.082	2.292	-0.877	0.397
	20	0.107	0.950	0.012	-0.117	1.155	-0.036	0.235	0.865	0.026	0.464	0.659	0.070	-0.334	1.305	-0.057	1.258	-0.014	0.212
	25	-0.018	1.029	-0.004	-0.290	1.248	-0.049	0.057	0.978	0.004	0.216	0.838	0.034	-0.154	1.136	-0.025	0.227	0.829	0.035
Midori. and Nogi 2015	5	0.367	0.361	0.540	0.446	0.338	0.512	0.310	0.513	0.422	0.502	0.347	0.492	0.294	0.501	0.456	0.555	0.366	0.445
	10	0.190	0.570	0.384	0.296	0.569	0.338	0.166	0.644	0.328	0.175	0.580	0.378	0.219	0.575	0.374	0.288	0.585	0.325
	15	0.082	0.724	0.262	0.149	0.681	0.273	0.092	0.786	0.202	0.084	0.737	0.248	0.093	0.712	0.272	0.133	0.785	0.180
	20	0.033	0.824	0.172	0.046	0.822	0.168	0.052	0.844	0.147	0.016	0.824	0.179	0.027	0.808	0.190	0.051	0.869	0.123
	25	0.008	0.908	0.092	0.011	0.884	0.112	0.010	0.927	0.074	0.008	0.907	0.093	0.005	0.909	0.093	0.021	0.921	0.076
Dai et al. 2013	5	0.525	0.845	-	0.619	0.784	-	0.570	0.837	-	0.693	0.770	-	0.632	0.825	-	0.885	0.677	-
	10	0.429	0.867	-	0.642	0.777	-	0.458	0.862	-	0.387	0.879	-	0.509	0.846	-	0.765	0.717	-
	15	0.312	0.901	-	0.465	0.837	-	0.418	0.866	-	0.321	0.894	-	0.340	0.900	-	0.844	0.674	-
	20	0.205	0.934	-	0.232	0.927	-	0.309	0.897	-	0.106	0.971	-	0.137	0.959	-	0.719	0.726	-
	25	0.112	0.962	-	0.203	0.925	-	0.150	0.949	-	0.078	0.973	-	0.055	0.985	-	0.522	0.800	-

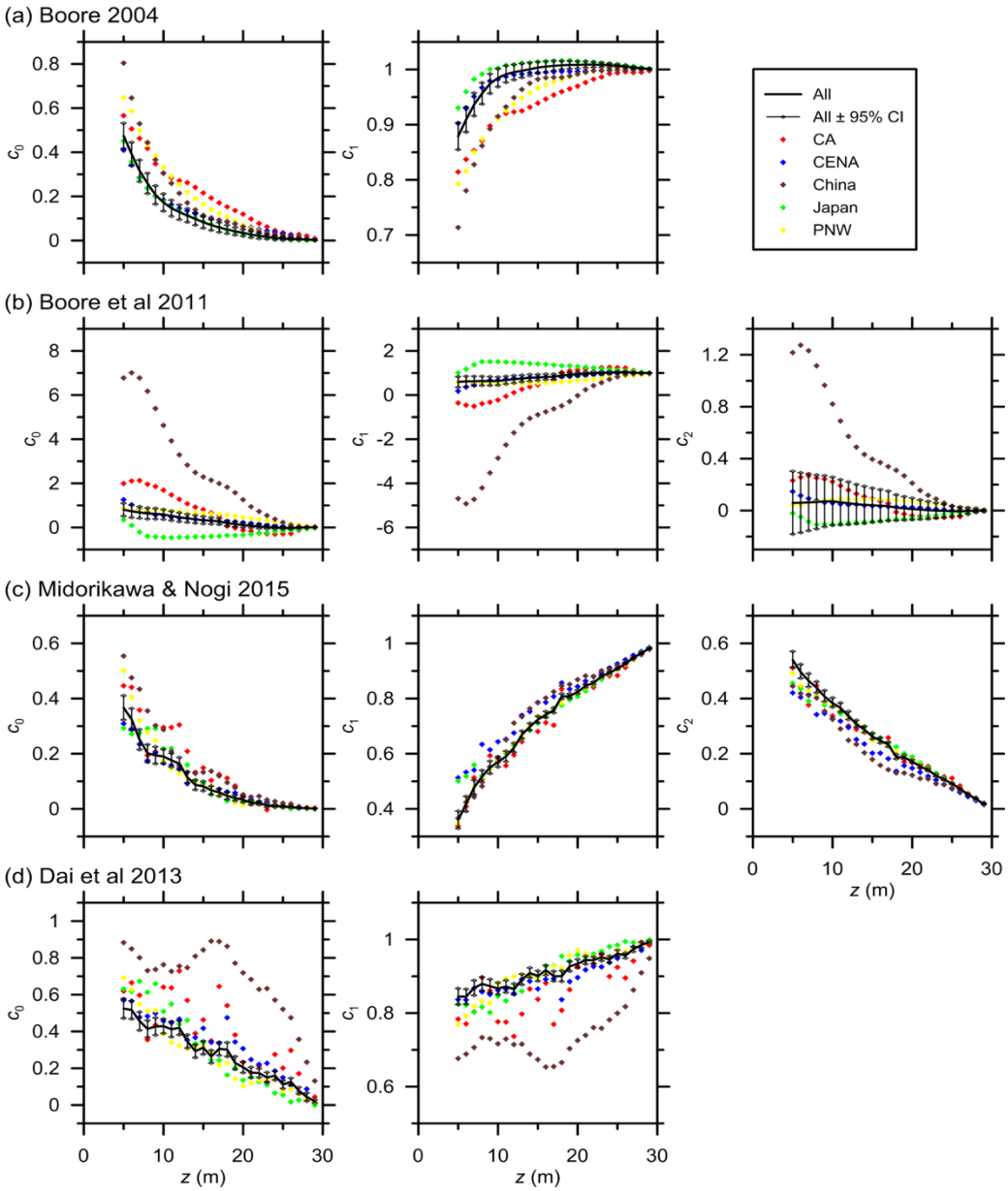

Figure 3. Depth-dependent model coefficients regressed with dataset for each region and with all datasets. Coefficients for (a) Boore (2004), (b) Boore et al (2011), (c) Midorikawa and Nogi (2015), and (d) Dai et al (2013). 95% confidence intervals of each coefficient are shown for all datasets only.

depths 5-29 m (1 m increment). Table 2 provides the model coefficients for profile depths of 5, 10, 15, 20, and 25 m.

We also developed non-region-specific coefficients for each functional form by combining all five data sets and assigning equal weights to each region in the regression. Figure 3 shows the non-region-specific coefficients (labelled as 'all') for each method with 95% confidence intervals; coefficients for each method are listed in Table 2.

All of the model coefficients exhibit regional variations, but these variations are more pronounced for some models than others. Based on visual inspection, Bea11 shows the greatest variations (Figure 3a), while MN15 have the smallest variations (Figure 3b). Coefficient c_2 in the Bea11 model as developed for 'All' (global dataset) has wide 95% confidence intervals, indicating that predicted V_{S30} is insensitive to c_2. B04 and Dea13 have similar regional variations of model coefficients (Figure 3 b and d), while Dea13 coefficients for CN are distinct from others (Figure 3d). This region-specific feature is discussed in Xie et al. (2016).

4 PERFORMANCE EVALUATION

Model performance is evaluated by analyzing residuals (R) as follows:

$$R = \ln(V_{S30}) - \ln(\widehat{V_{S30}}) \quad [7]$$

The mean (μ_R) and standard deviation (σ_R) of R are analyzed to evaluate model performance. Note that R is a measure of the difference between the predicted V_{S30} and the measured V_{S30}, and does not capture measurement error that needs to be considered separately. We do not consider measurement error in this study.

Figures 4 and 5 show μ_R and σ_R for each method and region, respectively. The μ_R for all methods and all regions are essentially zero, with the exception of WW15. This is expected because coefficients for B04, Bea11, MN15, and Dea13 were developed through regression analyses. This is not the case for the WW15. The μ_R of WW15 is less than 0.01 for profile depth (z) > 22 m for all regions, but it increases for smaller z.

MN15 and Dea13 show better performances than B04, Bea11, and WW15 for all regions and z ranges considered. MN15 and Dea13 provide approximately values of σ_R 30% lower than B04 and Bea11 for $z \geq 10$ m. The σ_R value for WW15 is comparable with those for the MN15 and Dea13 models if z > 22 m, but σ_R increases rapidly relative to other models with decreasing depth.

Residuals for CA, CENA, PNW, and JP have similar dispersions (σ_R = 0.1 to 0.2 at z = 10 m), but σ_R values for CN are significantly smaller (0.05 to 0.1 at z = 10 m). This is attributed to the similar geologic setting for CN sites, as described previously.

Non-region-specific (global) models are denoted with subscript 'All' (e.g., $MN15_{All}$, $Dea13_{All}$). Global model performance is investigated for MN15 and Dea13, which were selected because of their relatively favorable performance relative to other methods. We calculate residuals using regional datasets and the $MN15_{All}$ and $Dea13_{All}$ models. Figure 4f and 5f show μ_R and σ_R evaluated from the resulting residuals. Although the 'All' and regional model coefficients are different (Figure 3), μ_R values in Figure 4f are stable and σ_R values in Figure 5f are essentially the same as those for the region-specific models (Figure 5 a to e). As shown in Figure 4f, for $z \geq 20$ m, $\mu_R \sim 0$ and μ_R for z > 15 m is less than 0.02. CENA and JP have bias μ_R that increases with decreasing z, whereas CA, PNW, and China have the opposite trend. Values of σ_R increase slightly using $Dea13_{All}$ and $MN15_{All}$ (maximum $\Delta\sigma_R < 0.007$ for z = 5 – 29 m).

5 CONCLUSION

Five V_{SZ}-to-V_{S30} extrapolation models (Boore, 2004; Boore et al., 2011; Midorikawa and Nogi, 2015; Dai et al., 2013; Wang and Wang, 2015) have been evaluated using a V_S profile database compiled from profiles in California, Central and Eastern North America, Pacific Northwest, Japan, and China (total of 1,466 profiles). Region-specific model coefficients for B04, Bea11, MN15, and Dea13 were developed and a z_1-to-z_2 interval for WW15 was recommended. Model performance was evaluated from the mean and standard deviation of residuals. Among the considered models, MN15 and Dea13 provide the smallest dispersion, indicating better performance.

Non-region-specific models using Dea13 and MN15 methods ($MN15_{All}$ and $Dea13_{All}$) show good performance for profile depths (z) ≥ 15 m, with small bias and small dispersion increase relative to the respective regional models. The overall σ_R for z > 15 m is less than 0.15 in natural logarithmic unit, which is significantly lower than σ_R of geotechnical investigation or proxy-based V_{S30} estimation (usually in the range 0.25–0.50). The non-region-specific models are expected to provide robust V_{S30} prediction from V_S profiles with depth deeper than 15 m for all regions. Uncertainties increase markedly for shallower depths.

Models in this study are applicable to measured V_S

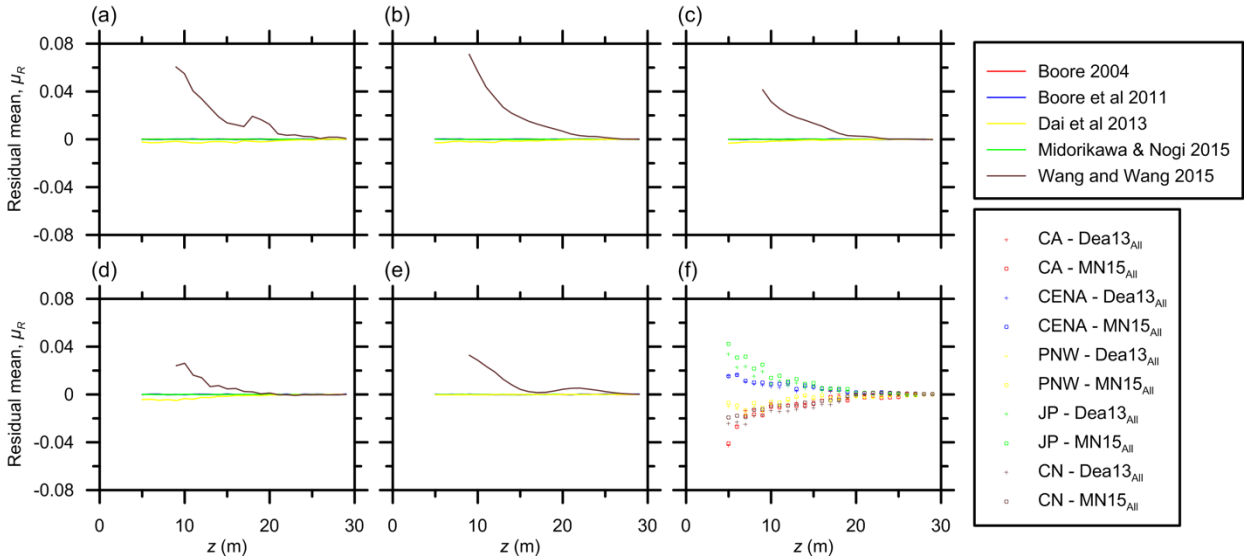

Figure 4. Mean of residuals applying five methods to regional dataset [i.e., (a) CA, (b) CENA, (c) PNW, (d) JP, and (e) CN] and (f) applying $Dea13_{All}$ and $MN15_{All}$ to each regional dataset.

profiles (or V_{SZ} values) for which exploration depth is shallower than 30 m. We note that MN15 and Dea13 provide better performance, but they require a V_S value at profile depth z and hence are most suitable when used in combination with V_S profiles from geophysical methods.

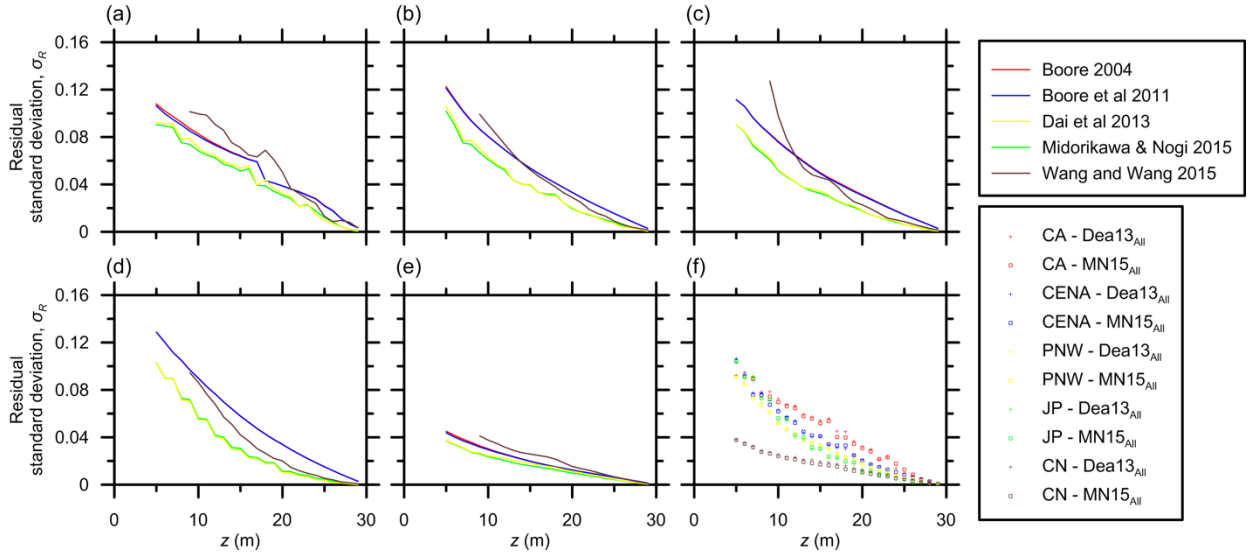

Figure 5. Standard deviation of residuals applying five methods to regional dataset [i.e., (a) CA, (b) CENA, (c) PNW, (d) JP, and (e) CN] and (f) applying Dea13$_{All}$ and MN15$_{All}$ to each regional dataset.

Geophysical measurements to depths of 30 m or greater are always preferred, and the availability of methods such as those presented here are not an excuse for limited exploration depths.

6 REFERENCES

Ahdi, S. K., J. P. Stewart, T. D. Ancheta, D. Y. Kwak, and D. Mitra (201x). Development of V_S profile database and proxy-based models for V_{S30} prediction in the Pacific Northwest region of North America, *Bull. Seism. Soc. Am.*, in-review.

Boore, D. M. (2004). Estimating V_{S30} (or NEHRP site classes) from shallow velocity models (depths < 30 m), *Bull. Seism. Soc. Am.*, **94**(2), 591–597.

Boore, D. M., E. M. Thompson, and H. Cadet (2011). Regional correlations of V_{S30} and velocities averaged over depths less than and greater than 30 meters, *Bull. Seism. Soc. Am.*, **101**(6), 3046–3059.

Brandenberg, S. J., N. Bellana, and T. Shantz (2010). Shear wave velocity as function of standard penetration test resistance and vertical effective stress at California bridge sites, *Soil Dyn. Earthq. Eng.* **30**, 1026–1035.

Cha, M., J. C. Santamarina, H. S. Kim, and G. C. Cho (2014). Small-strain stiffness, shear-wave velocity, and soil compressibility. *Journal of Geotechnical and Geoenvironmental Engineering*, **140**(10), 06014011.

Dai, Z., X. Li, and C. Hou (2013). A shear-wave velocity model for V_{S30} estimation based on a conditional independence property, *Bull. Seism. Soc. Am.*, **103**(6), 3354–3361.

Midorikawa, S. and Y. Nogi (2015). Estimation of V_{S30} from shallow velocity profile, *J. Japan Assoc. Earthq. Eng.*, **15**(2), 91–96 (in Japanese).

National Research Institute for Earth Science and Disaster Resilience (NIED) (2017). Strong-motion seismograph networks, http://www.kyoshin.bosai.go.jp

Port and Airport Research Institute (PARI) (2017). Strong-motion seismograph network for port regions, http://www.eq.pari.go.jp/kyosin/

Parker, G. A., J. A. Harmon, J. P. Stewart, Y. M. A. Hashash, A. R. Kottke, E. M. Rathje, W. J. Silva, and K. W. Campbell (2017). Proxy-based V_{S30} estimation in Central and Eastern North America, *Bull. Seism. Soc. Am.,* accepted.

Seyhan, E., J. P. Stewart, T. D. Ancheta, R. B. Darragh, and R. W. Graves (2014). NGA-West2 Site Database, *Earthq. Spectra*, **31**(3), 1007–1024.

Wang, H.-Y. and S.-Y. Wang (2015). A new method for estimating V_S(30) from a shallow shear-wave velocity profile (depth < 30 m), *Bull. Seism. Soc. Am.*, **105**(3), 1359–1370.

Xie, J., P. Zimmaro, X. Li, Z. Wen, and Y. Song (2016). V_{S30} empirical prediction relationships based on a new soil-profile database for the Beijing plain area, China, *Bull. Seism. Soc. Am*., **106**(6), 2843-2854.